Journal of Radiation Research, 2013, 54, 235–242
doi: 10.1093/jrr/rrs095 Advance Access Publication 7 November 2012

Effects of expression level of DNA repair-related genes involved in the NHEJ pathway on radiation-induced cognitive impairment

Li-Yuan ZHANG, Lie-Song CHEN, Rui SUN, Sheng-Jun JI, Yan-Yan DING, Jia WU and Ye TIAN*

Department of Radiotherapy and Oncology, The Second Affiliated Hospital of Soochow University, San Xiang Road No. 1055, Suzhou 215004, China
*Corresponding author: Tel: + 86-512-6778-3430; Fax: + 86-512-6828-4303; Email: dryetian@hotmail.com

(Received 29 April 2012; revised 6 September 2012; accepted 25 September 2012)

Cranial radiation therapy can induce cognitive decline. Impairments of hippocampal neurogenesis are thought to be a paramountly important mechanism underlying radiation-induced cognitive dysfunction. In the mature nervous system, DNA double-strand breaks (DSBs) are mainly repaired by non-homologous end-joining (NHEJ) pathways. It has been demonstrated that NHEJ deficiencies are associated with impaired neurogenesis. In our study, rats were randomly divided into five groups to be irradiated by single doses of 0 (control), 0 (anesthesia control), 2, 10, and 20 Gy, respectively. The cognitive function of the irradiated rats was measured by open field, Morris water maze and passive avoidance tests. Real-time PCR was also used to detect the expression level of DNA DSB repair-related genes involved in the NHEJ pathway, such as *XRCC4*, *XRCC5* and *XRCC6*, in the hippocampus. The influence of different radiation doses on cognitive function in rats was investigated. From the results of the behavior tests, we found that rats receiving 20 Gy irradiation revealed poorer learning and memory, while no significant loss of learning and memory existed in rats receiving irradiation from 0–10 Gy. The real-time PCR and Western blot results showed no significant difference in the expression level of DNA repair-related genes between the 10 and 20 Gy groups, which may help to explain the behavioral results, i.e. DNA damage caused by 0–10 Gy exposure was appropriately repaired, however, damage induced by 20 Gy exceeded the body's maximum DSB repair ability. Ionizing radiation-induced cognitive impairments depend on the radiation dose, and more directly on the body's own ability to repair DNA DSBs via the NHEJ pathway.

Keywords: DNA repair; DSB; radiation; XRCC4; XRCC5; XRCC6; cognitive impairments

INTRODUCTION

Radiation therapy (RT) is a very important treatment modality for cancer patients, but various adjacent normal tissue toxicities may occur after RT. Ionizing radiation may cause DNA clustered damaged sites (made up of double-strand breaks (DSBs) with associated base lesions, or abasic (AP) sites), and non-DSB clusters (comprised of base lesions, AP sites and single strand breaks) [1–3]. Without timely and accurate repair, even low-dose ionizing radiation may induce irreparable DNA damage that can lead to replicational and transcriptional errors, and thus cell apoptosis or disordered cell growth, resulting in premature aging, neurological disease or even cancer [4–6]. The nervous system is very sensitive to DNA damage, particularly in comparison with other non-replicating cell types; it is often profoundly affected by DNA repair deficiency, which can result in neurodegeneration [7]. Unrepaired DNA damage in the nervous system can be sufficient to cause cognitive decline [8]. It has been reported that deficiency in DNA damage repair, in both DNA single-strand breaks and DNA DSBs, can lead to neurological disease [9]. DSB is the most serious type of DNA damage and the unique cell-lethal one [10–12]. In the process of nucleotide excision repair (NER) and base excision DNA repair (BER) the undamaged strand could be used as a template to replicate. However, in DSB, both strands of DNA break simultaneously, which makes the DNA double-strand break repair (DSBR) more difficult to execute than other types of repair [13]. It is well known that, the H2AX histone protein is phosphorylated after DNA DSBs, and the protein gamma-H2AX (γ-H2AX) is taken as a marker of DNA DSBs [14]. The

repair of DSBs in human cells involves two different pathways: the homologous recombination repair (HR) and the non-homologous end-joining (NHEJ) pathways [15–16]. In non-replicating cells, such as those in the mature nervous system, DNA DSBs are mainly repaired by NHEJ [17–19]. NHEJ deficiencies in mice are associated with impaired neurogenesis [20–23]. Interestingly, impairments of hippocampal neurogenesis are thought to be a paramountly important mechanism underlying radiation-induced cognitive decline [24]. This may suggest that NHEJ plays an important role in radiation-induced cognitive impairments.

NHEJ of DNA DSBs is mediated by two protein complexes comprising XRCC5(Ku80)/XRCC6(Ku70)/DNA-PKcs/Artemis and XRCC4/LigaseIV/XLF [25]. Cells deficient in any of the NHEJ core proteins display pronounced hypersensitivity to ionizing radiation and a reduced ability to rejoin radiation-induced DSBs [26]. XRCC5/XRCC6 directly mediates incorporation of XRCC4 into end-joining complexes, and they are the core of the NHEJ reaction. Hence in our present study, the expression level of several DNA repair-related genes involved in the NHEJ pathway (XRCC4, XRCC5 and XRCC6) in the irradiated hippocampus was investigated to illustrate the relationship between the status of NHEJ and radiation-induced cognitive dysfunction.

MATERIALS AND METHODS

Animals

A total of 50 Sprague-Dawley rats (male, one month old) were obtained from the Experimental Animal Center of Soochow University, Suzhou, China. The animals were kept in a temperature- and light-controlled environment with a 12h/12h light/dark cycle, and provided with food and water *ad libitum*. The 50 rats were randomly divided into five groups to receive irradiation (IR) treatments with a single dose of 0 (control), 0 (anesthesia control), 2, 10 and 20 Gy, respectively. The Animal Care and Ethics Committee at the Soochow University, China, approved all experimental procedures.

Irradiation

The animals were anesthetized with 3.6% chloral hydrate (360 mg/kg, intraperitoneal injection). Then the whole brain was irradiated by use of 4-MeV electron beams delivered by a linear accelerator (Philips SL – 18) at room temperature, as described previously [27]. The rats in the anesthesia control group received 0 Gy of IR but underwent the same stress as did the others. The rats in the control group did not receive any treatment.

Cognitive test

A cognitive test was performed two months after IR. The sequence of behavioral testing was such that tests were administered in order of increasing stress level, and they included open field, Morris water maze and passive avoidance testing. All experiments were performed during 08:00–16:00, and the experimenter was blinded to the treatment given to the rats.

Open field test

The open field used in this experiment consisted of a perspex box (410 mm × 410 mm × 505 mm), closed with a sound-proof chamber. The open field was divided into 25 units of 8 cm squares: 4 squares in the corners, 12 squares in the surrounding portion, 8 squares in the middle and 1 square in the inner portion. The middle and inner area were called central region. Each session was started by placing the rat in the central area and rats were allowed to move freely around the open field and to explore the environment for 10 min. The path of the animals was recorded by the automated video-tracking system (Jiliang, Shanghai, China). The video-tracking program was used to measure the total distance traveled and the time spent in the central region of the open field. In order to eliminate any olfactory cues, the apparatus was cleaned with 10% ethanol after each individual test.

Morris water maze test

Rats were tested for spatial learning and memory using the Morris water maze, as described previously [28]. The Morris water maze consisted of a circular water tank (160 cm diameter, 49.5 cm height) that was partially filled with water (22 ± 1ºC) of 370 mm depth. The pool was divided (virtually) into four equal zones, labeled North/South/East/West. A platform (9 cm diameter) was placed in one of the four maze zones (the target zone) and submerged 1.5 cm below the water surface. The platform remained in the same zone during the entire experiment. The place navigation test was conducted on the Days 1 to 4, while the spatial probe test was performed on Day 5.

Place navigation test. The rats were required to find the platform using only the distal spatial cues available in the testing room. The cues were maintained constant throughout the test. There was a ceiling time of 60 s. The rat had to swim until it climbed onto the platform submerged underneath the water. After climbing onto the platform, the animal was permitted to remain there for 10 s before the commencement of the next trial. The escape platform was kept in the same position relative to the distal cues. If the rat failed to reach the escape platform within the maximally allowed time of 60 s, it was gently placed on the platform and allowed to remain there for 10s. The time to reach the platform ('latency') was measured. The same procedure was repeated for four trials per day. The latency and swim speed were recorded by the automated video-tracking system (Jiliang, Shanghai, China).

Spatial probe test. The hidden platform was removed on Day 5 of the water maze test, and then the rat was placed into the pool, as in the place navigation test, at a relatively constant position. The time for crossing the former platform zone, and the total time for crossing all zones were recorded for 30 s by the automated video-tracking system (Jiliang, Shanghai, China).

Passive avoidance test

The passive avoidance test was studied in a one-trial learning, step-through type of passive avoidance task. The apparatus consisted of two chambers having a steel-rod grid floor. One of the chambers (515 mm × 260 mm × 445 mm) was equipped with a lamp, located centrally at a height of 300 mm. The other was a dark chamber of the same size, connected through an arched door (5 × 5 cm). The apparatus was placed in a sound-proof chamber. When the rat was placed in the light chamber with its back to the door, it would eventually enter the dark chamber, owing to the natural preference of rats for a dark environment. When an inescapable, scrambled footshock (39 V, 50 Hz) was delivered through the grid floor in the dark chamber, the rat would escape from the dark chamber. Then the rat was put back into the home cage until the retention trial. Twenty-four hours later, the retention trial was carried out. The rat was again placed in the light chamber, as in the training trial, and the step-through latency was recorded by the automated video-tracking system (Jiliang, Shanghai, China). The upper cut-off time was 300 s. Before commencement of the next test, 10% ethanol was used to clean the equipment to eliminate odors.

Real-time PCR analysis of DNA repair-related genes

Two months after the treatment, each rat was killed to obtain the hippocampus. The total RNA was isolated from the hippocampus of each of the 50 rats using TRI-zol reagent (Molecular Research Center, Cincinnati, OH, USA). A 2-μg aliquot of the total RNA from each specimen was reverse-transcribed into single-strand cDNA using oligo primers and Su-perscriptII (Invitrogen, Carlsbad, CA, USA). The relative gene expression of *XRCC4*, *XRCC5* and *XRCC6* were determined using β-actin as an internal standard and the ABI Prism 7000 sequence detection system (Applied Biosystems, Foster City, CA, USA) based on the SYBR green method. The primer pairs used in the present study were as follows, for XRCC4, 5′-CTG AGG AGG ATG GGC TTT ATG AT-3′ (forward) and 5′-CAA GAT TTG TCT GCA TTC GGT GT-3′ (reverse); for XRCC5, 5′-AAA GAG TTG GGT AGT TGT GGA CGC A-3′ (forward) and 5′-TCC ATA GCG GAA CCC TTG AAT AG-3′ (reverse); for XRCC6, 5′-AAG AAT GTC TCC CCT TAT TTT GTG G-3′(forward) and 5′-TCT CGA AAC TGT CGC TCC TGT ATG T-3′(reverse); and for β-actin, 5′-GTT GAC ATC CGT AAA GAC C-3′(forward) and 5′-TAG GAG CCA GGG CAG TAA TC -3′ (reverse). The PCR reaction mixture (final volume 20 μl) contained 0.1 μM each primer, 10 μl × SYBR Premix EX Taq premix reagent (Perfect RealTime, Takara, Dalian, China), and 50 ng cDNA. The cycling conditions consisted of 95°C for 2 min, followed by 40 cycles of 95°C for 15 s and 60°C for 1 min. Expression of these genes in individual samples was normalized against that of β-actin using a modification of the method described by Lehmann and Kreip [29]. All analyses were performed in a blinded fashion, with laboratory personnel unaware of the IR dosage.

Western blot analysis

Western blot assays were performed to detect DSB repair-related genes and γ-H2AX expression in different IR cohorts. Of the 50 rat hippocampus tissues which had been harvested from rats two months after IR, 25 (5 of each cohort) were homogenized in 800 μl detergent lysis buffer. The tissue homogenates were then centrifuged at 12 000 g for 15 min to get the supernatant, and 60 μg of total proteins (the supernatant) were run on SDS-polyacrylamide gel electrophoresis (SDS-PAGE) and transferred to PVDF (Millipore, Billerica, MA, USA). The membrane was blocked with 5% milk in TBS with 0.05% Tween-20 for 1 h at room temperature, with constant agitation. The polyclonal antibody for XRCC4, XRCC5, XRCC6, γ-H2AX, and the monoclonal antibody for β-actin, were all purchased from Santa Cruz Biotechnology (Santa Cruz, CA, USA). The membranes were incubated overnight at 4°C with the primary antibody diluted 1:1000, and the proteins were detected with a Phototope-horseradish peroxidase Western blot detection kit (Cell Signaling Technology, Danvers, MA, USA). Optical band density was quantified (Imager of Alpha Corporation, San Leandro, CA, USA) and the results obtained for XRCC4, XRCC5, XRCC6 and γ-H2AX were normalized to that of β-actin.

Statistical analysis

All of the data were expressed in terms of mean ± SD and analyzed with single-element variance (One-way ANOVA) by SPSS16.0 software. A value of $P < 0.05$ was considered statistically significant.

RESULTS

General observation

All rats survived after the whole brain exposure. In the 20 Gy group, 3 rats displayed mild local skin reactions, excluding depilation, hyperemia, and edema at the irradiated area 10–50 days after IR. However, these conditions were not severe enough to prevent them from undergoing the behavioral tests and subsequent analysis. All rats performed normal daily activities, including feeding and drinking. No

paralysis or seizures were observed. Body weight in the 20 Gy group slightly decreased in the first month after IR but returned to normal quickly. The changes did not reach statistical significance, and there was no difference between the groups. Histologic examination of the rat brains obtained two months after IR revealed no gross morphologic changes such as demyelination, hemorrhage, or neuronal damage. This indicates that whole brain IR at a single dose of 2, 10, or 20 Gy couldn't induce any gross histologic change.

Cognitive test

The Morris water maze test, including the place navigation and the spatial probe test, was used to assess the acquisition and retention of spatial working memory and spatial reference memory, respectively. During the place navigation test, all rats significantly improved their performance, using their spatial working memory successfully. However, in the group given an IR exposure of 20 Gy, the latency time was significantly longer than for the other groups (20 Gy, 31.375 ± 2.085). There was no difference in latency between the other groups (C, 25.378 ± 1.375; S, 25.146 ± 1.883; 2 Gy, 21.533 ± 1.988; 10 Gy, 24.353 ± 1.800; Fig. 1A).

In the spatial probe test, all groups spent significantly more time in the target quadrant than in any other quadrant, but there was no difference between groups in the time spent in the target quadrant (C, 39.694 ± 2.536; S, 37.909 ± 1.726; 2 Gy, 40.484 ± 2.831; 10 Gy, 35.1403 ± 5.190; 20 Gy, 40.519 ± 2.752.), as shown in Fig. 1B. For all groups, there was no difference in the swimming speed.

The passive avoidance test was used to evaluate contextual learning and memory, and in this task, rats were trained to form an association between a foot-shock and the dark chamber. Two months after IR, there was no difference between the control and all the radiated groups with respect to latency before entering the dark chamber (Fig. 1C).

The open field test was used to assess locomotor, exploratory and anxiety-like behavior in rats. In this

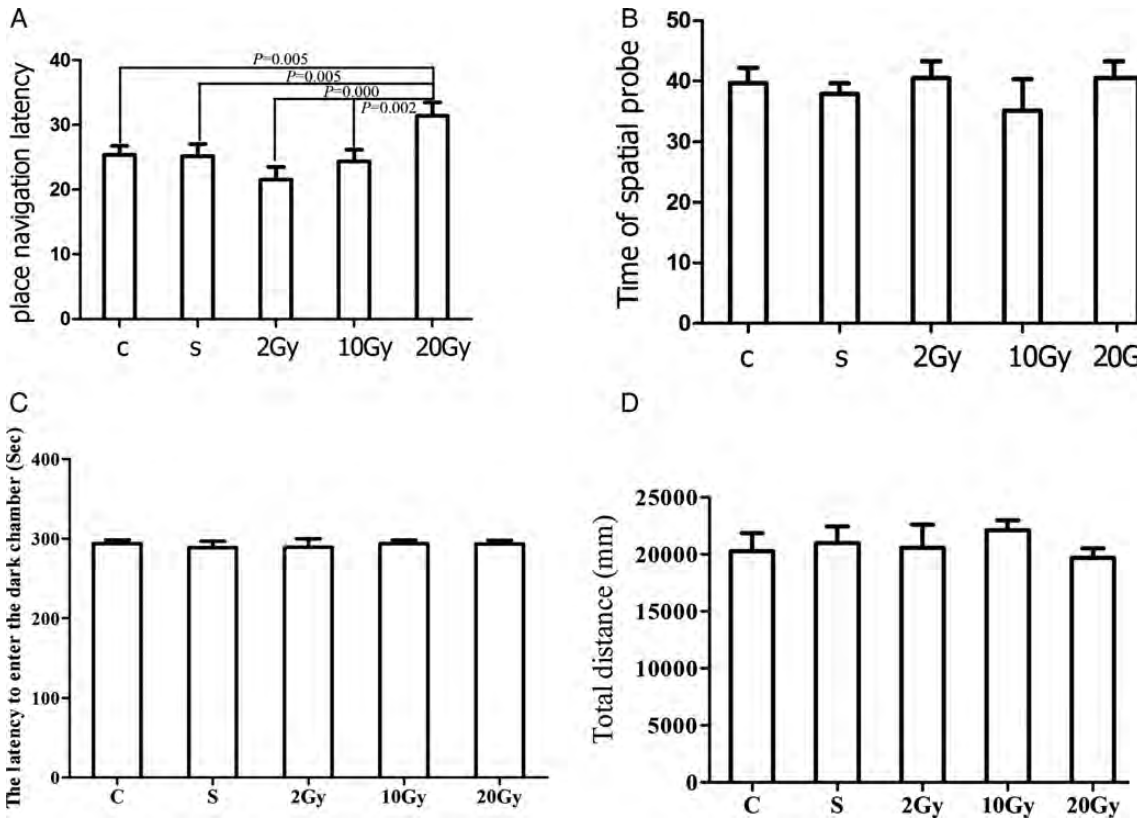

Fig. 1. Behavior results of rats two months after exposure to 0–20 Gy irradiation (IR). **A.** Effects of whole brain IR on rats' place navigation in Morris water mazes. Rats exposed to different doses of radiation were subjected to the Morris water maze test. The latency time was plotted and shown as indicated. **B.** Effects of whole brain IR on spatial probe in Morris water maze. The target quadrant staying time was plotted and shown as indicated. **C.** Effects of whole brain IR on rats' passive avoidance test. The latency to enter the dark chamber was plotted and shown as indicated. **D.** Effects on locomotor activity of rats exposed to different doses of radiation. The *y*-axis shows the total distance traveled by rats exposed to different doses of radiation in the open field test. The columns represent the mean value ± SEM for the five groups of rats.

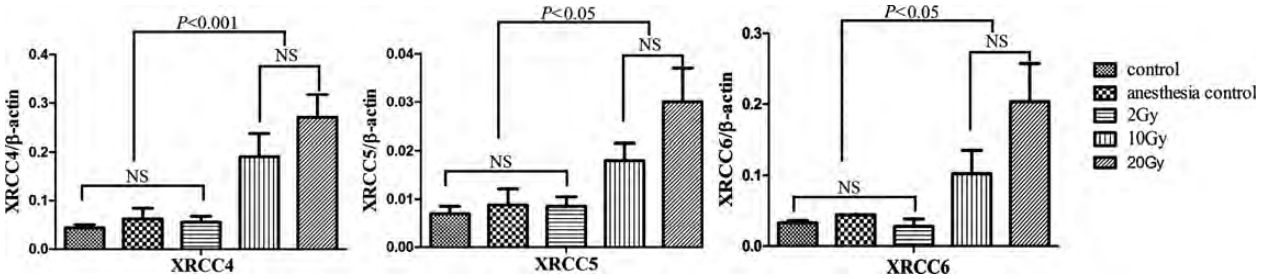

Fig. 2. Expression levels of XRCC4, XRCC5 and XRCC6 mRNA in rats' hippocampus two months after exposure to 0–20 Gy irradiation. The columns represent the mean value ± SEM for the five groups of rats. There was no difference in gene expression between the 10 Gy and 20 Gy groups.

experiment, there were no intergroup differences in the time spent in the central region, or in the total distance traveled, as shown in Fig. 1D. This suggests that ionizing radiation has no effect on locomotor activity or anxiety.

Real time PCR analysis of DNA repair-related genes

The expression of DNA repair-related genes in the rat hippocampus after different doses of IR were examined by real-time PCR. The results revealed that expression levels (normalized against β-actin) of *XRCC4* (C, 0.044 ± 0.0066; S, 0.0622 ± 0.0219; 2 Gy, 0.0555 ± 0.0122; 10 Gy, 0.191 ± 0.0465; 20 Gy, 0.271 ± 0.0473.), *XRCC5* (C, 0.007 06 ± 0.001 48; S, 0.008 86 ± 0.0033; 2 Gy, 0.008 54 ± 0.001 97; 10 Gy, 0.018 ± 0.003 55; 20 Gy, 0.03 ± 0.007 06.), *XRCC6* (C, 0.0329 ± 0.003 22; S, 0.0442 ± 0.008 99; 2 Gy, 0.0279 ± 0.0106; 10 Gy, 0.102 ± 0.0329; 20 Gy, 0.203 ± 0.054.) differs significantly between rats receiving 0 to 10 Gy IR (P = 0.015, 0.025, 0.038, for *XRCC4, XRCC5, XRCC6*), respectively. However, there exists no significant difference in the gene expression of rat hippocampus receiving 10 and 20 Gy IR (P = 0.277, 0.195, 0.139, for *XRCC4, XRCC5, XRCC6*, respectively) (Fig. 2).

Western blot analysis of XRCC4, XRCC5, XRCC6 and γ-H2AX

As shown in Fig. 3, 25 hippocampus tissues from rats with different doses of IR were examined by Western blot. We found that the trends of protein levels of DNA repair genes were consistent with the mRNA levels. The levels of XRCC4, XRCC5, XRCC6 and γ-H2AX protein in the 10 Gy IR group was significantly higher than that in the control group and the anesthesia control group (P = 0.006 and 0.011, P = 0.021 and 0.046, P = 0.035 and 0.039, P = 0.001 and 0.026, for XRCC4, XRCC5, XRCC6 and γ-H2AX respectively). When compared with the 2 Gy IR group, the levels of XRCC4, XRCC5, XRCC6 and γ-H2AX protein was still higher in the 10 Gy IR group (P = 0.029, P = 0.029, P = 0.049, P = 0.001). Similarly, all

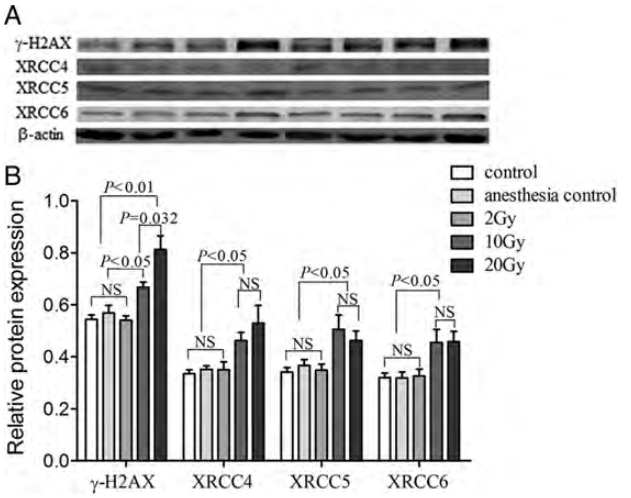

Fig. 3. The γ-H2AX, XRCC4, XRCC5 and XRCC6 protein expression levels in the rats' hippocampus. **A:** Protein expression levels in rat hippocampus tissues. The protein expression levels were normalized to that of β-actin by calculating the relative expression levels. Lane 1: control; lane 2: anesthesia control; lanes 3–4: 2 Gy; lanes 5–6: 10 Gy; lanes 7–8: 20 Gy. **B:** Analysis of protein levels in 25 rat hippocampus tissues from individuals that were treated with different doses of irradiation. The columns represent the mean value ± SEM for the five groups of rats.

of the protein levels of the 20 Gy IR group were higher than that of the control group, the anesthesia control group and the 2 Gy IR group (P = 0.024, 0.035 and 0.043, P = 0.019, 0.048 and 0.032, P = 0.012, 0.015 and 0.023, P = 0.001, 0.003 and 0.001 for XRCC4, XRCC5, XRCC6, respectively). There were no significant differences between the proteins levels of the 10 Gy IR group and the 20 Gy IR group (P = 0.402, P = 0.530, P = 0.961 for XRCC4, XRCC5 and XRCC6, respectively) except for γ-H2AX (P = 0.032) (Fig. 3B).

DISCUSSION

In this study, we investigated the influence of different doses of ionizing radiation on the nervous system, mainly

on cognitive function in rats. Using open field, Morris water maze and passive avoidance tests, we found that cranial IR of relative low-dose (lower than 10 Gy) radiation doesn't affect a rat's ability to repair DSB and its cognitive function. However, higher dose radiation (20 Gy) may induce damages exceeding the rat's DSB repair ability, and ultimately harm the nervous system, resulting in poorer spatial learning and memory. The behavior testing results were further confirmed by real-time PCR and Western blot detection, in which we found that the expression level of several DNA repair-related genes involved in the NHEJ pathway varies significantly between rats receiving 0 and 10 Gy IR. We found no significant difference in the expression level between rats receiving 10 and 20 Gy IR, indicating a limit for the rat's DNA damage repair ability over 10 Gy.

The global annual incidence of squamous cell carcinoma of the head and neck (SCCHN) and primary brain tumor have been estimated at 800 000 [30]. RT plays an important role in the curative and palliative treatment of patients with SCCHN, primary and metastatic brain tumors. The tolerance of brain tissues limits the radiation dose than can be delivered safely during cranial RT, and one of the potential complications that can arise involves cognitive dysfunction. The cognitive changes associated with cranial RT are typically subtle, and occur across various domains of cognition, including short-term memory and frontal functions—such as executive functions, attention, and analogical judgment. These symptoms appear several months to years following radiation exposure and worsen progressively, and they inevitably affect quality of life [31]. However, the underlying mechanisms for these effects are still elusive. The sensitivity of tissues to ionizing radiation varies significantly, and in the past the adult brain was considered to be insensitive to ionizing radiation. However, recent studies indicate the hippocampus in the adult brain is sensitive and may play an important role in radiation-induced cognitive dysfunction [32]. Consequently, we focused on the hippocampus in the present study, and the relationship between radiation and hippocampus damage was investigated. Furthermore, radiation-induced cognitive dysfunction includes impairments of learning, memory and emotion [33–35]. Accordingly, the irradiated rats' cognitive function was measured by Morris water maze, passive avoidance, and open field tests.

Although the mechanisms for ionizing radiation-induced cognitive impairments are not yet understood fully, neurogenesis of the hippocampus is likely to participate in morbidity. In many experimental studies ionizing radiation has been regarded as a classical means of inhibiting neurogenesis [36–37]. There is much research to show that the NHEJ core proteins are related to neurogenesis of the hippocampus [23].

The NHEJ pathway is the major DSB repair pathway in eukaryotes, and it can make corresponding modification and random connections in both ends of damaged DNA in the absence of homologous end sequences [17]. The process of NHEJ is as follows: firstly, a heterodimer called KU, formed by Ku80 (encoded by *XRCC5*) and Ku70 (encoded by *XRCC6*), recognizes a DSB site and binds to the DNA ends of the fracture to protect the free DNA sites from being broken down by nucleic acid enzymes; then, the DNA-PKcs, XRCC4/LIG4, is recruited to activate DNA-PK, and finally both ends of the fracture can be directly connected to repair the DSB (after a certain degree of decomposition processing). So, it can be inferred that all genes involved in this process, including XRCC4, XRCC5, XRCC6, LIG4 and DNA-PKcs, play very important roles in the DSB NHEJ repair process, and that defects in these genes might affect DNA repair, leading to increased genomic instability and even some diseases. For example, it has been found that *XRCC5* and *XRCC6* knockout mice show severe combined immunodeficiency (SCID) and higher sensitivity to ionizing radiation [38]. Barnes *et al*. also reported that *XRCC4* and *LiG4* knockout mice exhibit embryonic lethality or growth retardation, developmental stagnation, nerve cell apoptosis and immune deficiency [39]. *In vivo* and *in vitro* data reveal that XRCC4 directly interacts with XRCC5/XRCC6, which may be required for all productive NHEJ complexes [40]. Accordingly, XRCC4, XRCC5, and XRCC6 are the core of DNA DSB repair-related genes involved in the NHEJ pathway.

This is, to some extent, in line with our real-time PCR and Western blot results, i.e. expression of XRCC4, XRCC5 and XRCC6 in the hippocampus varied significantly between rats receiving 0 or 10 Gy of IR. However, we found no significant difference in XRCC4, XRCC5 and XRCC6 expression between the 10 Gy and 20 Gy groups. In addition, as a marker of DNA DSBs, the protein γ-H2AX showed significantly different expression levels in the hippocampus of rats receiving 0 and 20 Gy of IR. That is, as the IR dose increased, the γ-H2AX level went up. Moreover, it appears that there was a positive correlation between enhanced XRCC4, XRCC5 and XRCC6 levels and the γ-H2AX level. But after exceeding 10 Gy, the XRCC4, XRCC5 and XRCC6 levels can't be further enhanced with increase of the γ-H2AX level. There are the interdependence of NHEJ proteins for accumulation on DSBs between XRCC5(Ku80)/XRCC6(Ku70) and XRCC4 [40]. Therefore, we conclude that a higher dose of radiation (e.g. 20 Gy in our experiments) may cause so much or such severe DNA damage that the rat's defence mechanisms can't repair it and the nervous system will be affected.

In the present study, two months after IR, the 20 Gy group showed significant cognitive impairments in the Morris water maze (Fig. 1A). That is, 20 Gy radiation (the

higher dose) may have induced damage exceeding the rat's ability to repair DSBs, and hence produced cognitive dysfunction. Consistently, our Western blot results also revealed that the 20 Gy group had a higher level of expression of γ-H2AX (a marker of DNA DSBs) (Fig. 3). Other researchers have undertaken similar investigations. Raber *et al.* gave 2 month-old mice 10 Gy whole brain radiation exposure, and 3 months later, in the Morris water maze test there was no significant difference between the radiation group and the control group [41]. Another study, using IR at higher single doses, i.e. 20 Gy, revealed deficits in the Morris water maze tests [42].

Our results showed that there were no intergroup differences in the results for the open field test or the passive avoidance test, indicating that radiation doesn't impair anxiety or contextual memory, which is also in accordance with the results of others. In Madsen's study, mice irradiated by 24 Gy whole brain IR didn't show an abnormal anxiety level [43]. Clark *et al.* gave mice 15 Gy IR, and observed no impairment in contextual memory [44]. The cognitive tests indicate we have established an effective model to study radiation-induced cognitive dysfunction in the rat.

To our knowledge, this is the first study on the effects of the expression level of DNA repair-related genes involved in the NHEJ pathway on radiation-induced cognitive impairments. Our study has demonstrated that radiation-induced cognitive dysfunction in rats is dose-dependent, and that a single-dose exposure of 20 Gy is sufficient to induce cognitive dysfunction in rats. In addition, differences in DSB repair-related gene expression levels suggest that damages induced by 20 Gy IR might exceed the rat's repair ability, and lead to irreversible cognitive impairments.

In summary, ionizing radiation-induced cognitive impairments depend on radiation dose, and more directly on the limited capacity of the DNA DSB repair system involving the NHEJ pathway.

FUNDING

This study was supported by the National Natural Scientific Foundation of China grants 81172128 (Y.T.) and 81102077 (L.-Y.Z.); Jiangsu Province's Key Medical Department in 2011 (Y.T.); Project of Postgraduate's Innovation of Jiangsu Province cx10b-055z (L.-Y.Z).

REFERENCES

1. O'Neill P, Wardman P. Radiation chemistry comes before radiation biology. *Int J Radiat Biol* 2009;**85**:9–25.
2. Eccles LJ, O'Neill P, Lomax ME. Delayed repair of radiation induced clustered DNA damage: friend or foe? *Mutat Res* 2011;**711**:134–41.
3. Shikazono N, Noguchi M, Fujii K *et al*. The yield, processing, and biological consequences of clustered DNA damage induced by ionizing radiation. *J Radiat Res* 2009;**50**:27–36.
4. Pollard JM, Gatti RA. Clinical radiation sensitivity with DNA repair disorders: an overview. *Int J Radiat Oncol Biol Phys* 2009;**74**:1323–31.
5. Blundred RM, Stewart GS. DNA double-strand break repair, immunodeficiency and the RIDDLE syndrome. *Expert Rev Clin Immunol* 2011;**7**:169–85.
6. Jeppesen DK, Bohr VA, Stevnsner T. DNA repair deficiency in neurodegeneration. *Prog Neurobiol* 2011;**94**:166–200.
7. McKinnon PJ. DNA repair deficiency and neurological disease. *Nat Rev Neurosci* 2009;**10**:100–12.
8. Borgesius NZ, de Waard MC, van der Pluijm I *et al*. Accelerated age-related cognitive decline and neurodegeneration, caused by deficient DNA repair. *J Neurosci* 2011;**31**:12543–53.
9. Subba Rao K. Mechanisms of disease: DNA repair defects and neurological disease. *Nat Clin Pract Neurol* 2007;**3**:162–72.
10. Phillips ER, McKinnon PJ. DNA double-strand break repair and development. *Oncogene* 2007;**26**:7799–808.
11. Katyal S, McKinnon PJ. DNA strand breaks, neurodegeneration and aging in the brain. *Mech Ageing Dev* 2008; **129**:483–91.
12. Frappart PO, McKinnon PJ. Mouse models of DNA double-strand break repair and neurological disease. *DNA Repair (Amst)* 2008;**7**:1051–60.
13. Kass EM, Jasin M. Collaboration and competition between DNA double-strand break repair pathways. *FEBS Lett* 2010;**584**:3703–8.
14. Ford EC, Achanta P, Purger D *et al*. Localized CT-guided irradiation inhibits neurogenesis in specific regions of the adult mouse brain. *Radiat Res* 2011;**175**:774–83.
15. Ferguson DO, Alt FW. DNA double strand break repair and chromosomal translocation: lessons from animal models. *Oncogene* 2001;**20**:5572–9.
16. Nagasawa H, Brogan JR, Peng Y *et al*. Some unsolved problems and unresolved issues in radiation cytogenetics: a review and new data on roles of homologous recombination and non-homologous end joining. *Mutat Res* 2010;**701**:12–22.
17. Lieber MR, Ma Y, Pannicke U *et al*. Mechanism and regulation of human non-homologous DNA end-joining. *Nat Rev Mol Cell Biol* 2003;**4**:712–20.
18. Cromie GA, Connelly JC, Leach DR. Recombination at double-strand breaks and DNA ends: conserved mechanisms from phage to humans. *Mol Cell* 2001;**8**:1163–74.
19. Leong T, Chao M, Bassal S *et al*. Radiation-hypersensitive cancer patients do not manifest protein expression abnormalities in components of the nonhomologous end-joining (NHEJ) pathway. *Br J Cancer* 2003;**88**:1251–5.
20. Frank KM, Sharpless NE, Gao Y *et al*. DNA ligase IV deficiency in mice leads to defective neurogenesis and embryonic lethality via the pp53 pathway. *Mol Cell* 2000;**5**: 993–1002.
21. Gu Y, Sekiguchi J, Gao Y *et al*. Defective embryonic neurogenesis in Ku-deficient but not DNA-dependent protein kinase catalytic subunit-deficient mice. *Proc Natl Acad Sci U S A* 2000;**97**:2668–73.

22. Niimi N, Sugo N, Aratani Y *et al*. Genetic interaction between DNA polymerase beta and DNA-PKcs in embryogenesis and neurogenesis. *Cell Death Differ* 2005;**12**: 184–91.
23. Gao Y, Sun Y, Frank KM *et al*. A critical role for DNA end-joining proteins in both lymphogenesis and neurogenesis. *Cell* 1998;**95**:891–902.
24. Monje M, Dietrich J. Cognitive side effects of cancer therapy demonstrate a functional role for adult neurogenesis. *Behav Brain Res* 2012;**227**:376–9.
25. Schulte-Uentrop L, El-Awady RA, Schliecker L *et al*. Distinct roles of XRCC4 and Ku80 in non-homologous end-joining of endonuclease- and ionizing radiation-induced DNA double-strand breaks. *Nucleic Acids Res* 2008;**36**:2561–9.
26. Kasten-Pisula U, Tastan H, Dikomey E. Huge differences in cellular radiosensitivity due to only very small variations in double-strand break repair capacity. *Int J Radiat Biol* 2005;**81**:409–19.
27. Tian Y, Shi Z, Yang S *et al*. Changes in myelin basic protein and demyelination in the rat brain within 3 months of single 2-, 10-, or 30-Gy whole-brain radiation treatments. *J Neurosurg* 2008;**109**:881–8.
28. Vorhees CV, Williams MT. Morris water maze: procedures for assessing spatial and related forms of learning and memory. *Nat Protoc* 2006;**1**:848–58.
29. Lehmann U, Kreipe H. Real-time PCR analysis of DNA and RNA extracted from formalin-fixed and paraffin-embedded biopsies. *Methods* 2001;**25**:409–18.
30. Ferlay J, Shin HR, Bray F *et al*. Estimates of worldwide burden of cancer in 2008: GLOBOCAN 2008. *Int J Cancer* 2010;**127**:2893–917.
31. Soussain C, Ricard D, Fike JR *et al*. CNS complications of radiotherapy and chemotherapy. *Lancet* 2009;**374**:1639–51.
32. Fike JR. Physiopathology of radiation-induced neurotoxicity. *Rev Neurol (Paris)* 2011;**167**:746–50.
33. Shi L, Adams MM, Long A *et al*. Spatial learning and memory deficits after whole-brain irradiation are associated with changes in NMDA receptor subunits in the hippocampus. *Radiat Res* 2006;**166**:892–9.
34. Kiskova J, Smajda B. Open field behavior and habituation in rats irradiated on the head with gamma-rays. *Acta Physiol Hung* 2008;**95**:307–12.
35. Tomasova L, Smajda B, Bona M. Avoidance behaviour and anxiety in rats irradiated with a sublethal dose of gamma-rays. *Acta Biol Hung* 2011;**62**:341–8.
36. Kitamura T, Saitoh Y, Takashima N *et al*. Adult neurogenesis modulates the hippocampus-dependent period of associative fear memory. *Cell* 2009;**139**:814–27.
37. Snyder JS, Soumier A, Brewer M *et al*. Adult hippocampal neurogenesis buffers stress responses and depressive behaviour. *Nature* 2011;**476**:458–61.
38. Frank KM, Sekiguchi JM, Seidl KJ *et al*. Late embryonic lethality and impaired V(D)J recombination in mice lacking DNA ligase IV. *Nature* 1998;**396**:173–7.
39. Barnes DE, Stamp G, Rosewell I *et al*. Targeted disruption of the gene encoding DNA ligase IV leads to lethality in embryonic mice. *Curr Biol* 1998;**8**:1395–8.
40. Mari PO, Florea BI, Persengiev SP *et al*. Dynamic assembly of end-joining complexes requires interaction between Ku70/80 and XRCC4. *Proc Natl Acad Sci U S A* 2006;**103**: 18597–602.
41. Raber J, Rola R, LeFevour A *et al*. Radiation-induced cognitive impairments are associated with changes in indicators of hippocampal neurogenesis. *Radiat Res* 2004;**162**:39–47.
42. Hodges H, Katzung N, Sowinski P *et al*. Late behavioural and neuropathological effects of local brain irradiation in the rat. *Behav Brain Res* 1998;**91**:99–114.
43. Madsen TM, Kristjansen PE, Bolwig TG *et al*. Arrested neuronal proliferation and impaired hippocampal function following fractionated brain irradiation in the adult rat. *Neuroscience* 2003;**119**:635–42.
44. Clark PJ, Brzezinska WJ, Thomas MW *et al*. Intact neurogenesis is required for benefits of exercise on spatial memory but not motor performance or contextual fear conditioning in C57BL/6J mice. *Neuroscience* 2008;**155**:1048–58.